

# PiRank: Learning To Rank via Differentiable Sorting

Robin Swezey<sup>1</sup>, Aditya Grover<sup>2</sup>, Bruno Charron<sup>1</sup>, Stefano Ermon<sup>3</sup>

<sup>1</sup>Rakuten, Inc.

<sup>2</sup>Facebook AI Research

<sup>3</sup>Stanford University

{rswezey, bcharron}@acm.org, adityagrover@fb.com, ermon@cs.stanford.edu

## Abstract

A key challenge with machine learning approaches for ranking is the gap between the performance metrics of interest and the surrogate loss functions that can be optimized with gradient-based methods. This gap arises because ranking metrics typically involve a sorting operation which is not differentiable w.r.t. the model parameters. Prior works have proposed surrogates that are loosely related to ranking metrics or simple smoothed versions thereof. We propose PiRank, a new class of differentiable surrogates for ranking, which employ a continuous, temperature-controlled relaxation to the sorting operator. We show that PiRank exactly recovers the desired metrics in the limit of zero temperature and scales favorably with the problem size, both in theory and practice. Empirically, we demonstrate that PiRank significantly improves over existing approaches on publicly available internet-scale learning-to-rank benchmarks.

## 1 Introduction

The goal of Learning-To-Rank (LTR) models is to rank a set of candidate items for any given search query according to a preference criterion [1]. The preference over items is specified via relevance labels for each candidate. The fundamental difficulty in LTR is that the downstream metrics of interest (e.g., mean reciprocal rank (MRR), normalized discounted cumulative gain (NDCG) etc.) depend on the ranks (i.e. ordering) induced by the model. These ranks are not differentiable with respect to the model parameters, so the metrics cannot be optimized directly via gradient-based methods.

To resolve the above challenge, a popular class of LTR approaches map items to real-valued scores and then define surrogate loss functions that operate directly on these scores. Surrogate loss functions, in turn, can belong to one of three types. LTR models optimized via *pointwise* surrogates [2–5] cast ranking as a regression/classification problem, wherein the labels of items are given by their individual relevance labels. Such approaches do not directly account for any inter-dependencies across item rankings. *Pairwise* surrogate losses [6–13] can be decomposed into terms that involve scores of pairs of items in a list and their relative ordering.

Finally, *listwise* surrogate losses [14–18] are defined with respect to scores for an entire ranked list. For many prior surrogate losses, especially those used for listwise approaches, the functional form is inspired via downstream ranking metrics, such as NDCG. However, the connection is loose or heuristically driven. For instance, SoftRank [13, 18] learns a Gaussian distribution over scores, which in turn defines a distribution over ranks and the surrogate is the expected NDCG w.r.t. this rank distribution.

We propose PiRank, a listwise approach where the scores are learned via deep neural networks and the surrogate loss is obtained via a differentiable relaxation to the sorting operator. In particular, our approach extends the temperature-controlled NeuralSort [19] relaxation for sorting to commonly used ranking metrics such as NDCG and ARP. The resulting training objective for PiRank reduces to the exact metric optimization in the limit of zero temperature and trades off bias for lower variance in the gradient estimates when the temperature is high. Furthermore, we also propose a scalable variant of PiRank for real-world industrial scenarios where the overall size of the item lists is large but the ranking metrics of interest are determined by only a small set of top ranked items. Scaling is enabled by a divide-and-conquer strategy akin to merge sort, where we recursively apply the sorting relaxation to sub-lists of smaller size and propagate only the top items from each sub-list for further sorting.

Empirically, we test PiRank on two of the largest publicly available LTR datasets: MSLR-WEB30K [20] and Yahoo! C14. We find that PiRank significantly outperforms competing methods on these benchmarks on 14/18 ranking metrics and their variants, and is able to scale to very large item lists. Finally, we provide an open-source implementation<sup>1</sup> based on TensorFlow Ranking [21].

## 2 Preliminaries

The LTR setting considers a finite dataset consisting of  $n$  triplets  $D = \{q_i, \{\mathbf{x}_{i,j}\}_{j=1}^L, \{y_{i,j}\}_{j=1}^L\}_{i=1}^n$ . The  $i$ -th triplet consists of a query  $q_i \in \mathcal{Q}$ , a list of  $L$  candidate items represented as feature vectors  $\mathbf{x}_{i,j} \in \mathcal{X}$ , and query-specific relevance labels  $y_{i,j}$  for each item  $j$ . The relevance labels  $y_{i,j}$  can be binary, ordinal or real-valued for more fine-grained relevance. For generality, we focus on the real-valued setting.

<sup>1</sup><https://github.com/ermongroup/pirank>

Given a training dataset  $D$ , our goal is to learn a mapping from queries and itemsets to rankings. A ranking  $\pi$  is a list of unique indices from  $\{1, 2, \dots, L\}$ , or equivalently a permutation, such that  $\pi_j$  is the index of the item ranked in  $j$ -th position. Without loss of generality, we assume lower ranks (starting from 1) have higher relevance scores. This is typically achieved by learning a scoring function  $f : \mathcal{Q} \times \mathcal{X}^L \rightarrow \mathbb{R}^L$  that maps a query context and list of candidate items to  $L$  scores. At test time, the candidate items are ranked by sorting their predicted scores in descending order. The training of  $f$  itself can be done by a suitable differentiable surrogate objective, which we discuss next.

## 2.1 Surrogate Objectives for LTR

In this section, we briefly summarize prominent LTR approaches with a representative loss function for each category of pointwise, pairwise or listwise surrogate losses. We refer the reader to the excellent survey by [22] for a more extensive review. Omitting the triplet index, we denote the relevance labels vector as  $\mathbf{y} \in \mathbb{R}^L$  and an LTR model's score vector obtained via  $f$  as  $\hat{\mathbf{y}} \in \mathbb{R}^L$ .

The simplest pointwise surrogate loss for ranking is the mean-squared error (MSE) between  $\mathbf{y}$  and  $\hat{\mathbf{y}}$ :

$$\hat{\ell}_{\text{MSE}}(\mathbf{y}, \hat{\mathbf{y}}) = \frac{1}{L} \sum_{i=1}^L (\hat{y}_i - y_i)^2. \quad (1)$$

As the example loss above shows, pointwise LTR approaches convert ranking into a regression problem over the relevance labels and do not account for the relationships between the candidate items. Pairwise approaches seek to remedy this by considering loss terms depending in the predicted scores of pairs of items. For example, the widely used RankNet [8] aims to minimize the number of inversions, or incorrect relative orderings between pairs of items in the predicted ranking. It does so by modeling the probability  $\hat{p}_{i,i'}$  that the relevance of the  $i$ -th item is higher than that of the  $i'$ -th item as a logistic map of their score difference, for all candidate items  $i, i'$ . The objective is then the cross entropy:

$$\hat{\ell}_{\text{RankNet}}(\mathbf{y}, \hat{\mathbf{y}}) = - \sum_{i=1}^L \sum_{i'=1}^L \mathbb{1}(y_i > y_{i'}) \log \hat{p}_{i,i'} \quad (2)$$

where  $\mathbb{1}(\cdot)$  denotes the indicator function and  $\hat{p}_{i,i'}$  is a function of  $\hat{\mathbf{y}}$ . Pairwise approaches effectively model relationships between pairs of items and generally perform better than pointwise approaches, but still manifest limitations on downstream metrics which consider rankings in the full list and not just pairs. In fact, the larger the list of candidate items, the weaker these approaches tend to be: an error between the first and last item on a list is weighed the same in the RankNet loss as one between two neighboring items.

Listwise approaches take the further step to learn from errors on the complete list. LambdaRank [12] extends RankNet by assigning weights to every loss term from Eq. 2:

$$\hat{\ell}_{\text{LambdaRank}}(\mathbf{y}, \hat{\mathbf{y}}) = - \sum_{i=1}^L \sum_{i'=1}^L \Delta \ell_{\text{NDCG}}(i, i') \log \hat{p}_{i,i'} \quad (3)$$

with  $\Delta \ell_{\text{NDCG}}(i, i')$  the difference in the downstream metric NDCG (defined below) when swapping items  $i$  and  $i'$ .

## 2.2 Ranking Metrics

Downstream metrics operate directly on the predicted ranking  $\hat{\pi}$  (obtained by sorting  $\hat{\mathbf{y}}$  in descending order) and the true relevance labels  $\mathbf{y}$ . They differ from conventional metrics used for other supervised learning problems in explicitly weighting the loss for each item by a suitably chosen increasing function of its predicted rank. For example, relevance position (RP) [23] multiplies the relevance labels with linearly increasing weights, and normalizes by the total relevance score for the query:

$$\text{RP}(\mathbf{y}, \hat{\pi}) = \frac{\sum_{j=1}^L y_{\hat{\pi}_j} j}{\sum_{j=1}^L y_j} \quad (4)$$

Averaging RP across the predictions made for all the queries in the test set gives the average relevance position (ARP) metric. Lower ARP signifies better performance.

A very common metric is the discounted cumulative gain (DCG) [24]. DCG computes the rescaled relevance of the  $j$ -th candidate by exponentiating its relevance label, and further divides it by the assigned log-ranking. This model incentivizes ranking models to focus on elements with higher graded relevance scores:

$$\text{DCG}(\mathbf{y}, \hat{\pi}) = \sum_{j=1}^L \frac{2^{y_{\hat{\pi}_j}} - 1}{\log_2(1 + j)} \quad (5)$$

A more common variant NDCG normalizes DCG by the maximum possible DCG attained via the optimal ranking  $\pi^*$  (obtained by sorting  $\mathbf{y}$  in descending order):

$$\text{NDCG}(\mathbf{y}, \hat{\pi}) = \frac{\text{DCG}(\mathbf{y}, \hat{\pi})}{\text{DCG}(\mathbf{y}, \pi^*)} \quad (6)$$

Higher DCG and NDCG signify better performance. Their truncated versions  $\text{DCG}@k$  and  $\text{NDCG}@k$  are defined by replacing  $L$  with a cutoff  $k$  in Eq. 5 so metrics are computed on the top- $k$  items.

## 3 PiRank

In PiRank, we seek to design a new class of surrogate objectives for ranking that address two key challenges with current LTR approaches. The first challenge is the statistical gap between the downstream ranking metric of interest (e.g., NDCG, ARP) that involve a non-differentiable sorting operator and the differentiable surrogate function being optimized. The second challenge concerns the scalability w.r.t. the size of the candidate list  $L$  for each query item. Larger list sizes are standard in industrial applications but present computational and memory challenges for current approaches during both training and test-time inference. Pairwise and listwise methods (or hybrids) typically scale quadratically in the list size  $L$ , the number of items to rank for each query. Combining surrogates for truncated metrics, such as LambdaRank in Eq. 3 with  $\text{NDCG}@k$  has a reduced complexity of  $O(kL)$  but comes at the cost of vanishing gradient signal

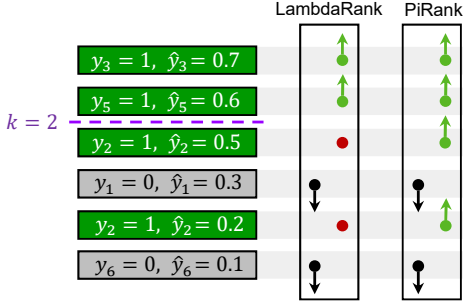


Figure 1: A set of items, green if relevant and gray otherwise, sorted by their score. Arrows show the sign of the loss derivative w.r.t. each item’s predicted score for different methods (positive for black, negative for green and zero for red dots). Pairwise approaches weighted by differences in truncated ranking metrics, such as LambdaRank with NDCG@ $k$  as illustrated, would put zero weights on the relevant items ranked above  $k = 2$ , thus bypassing learning signal. In comparison, PiRank efficiently learns from all items even using a  $k = 2$  truncated loss.

from relevant entries below  $k$  (see Figure 1 for an illustration). Soft versions of the truncation metrics, such as Approximate NDCG Loss [25], can fully learn from all items but again scale quadratically with  $L$  or do not take advantage of GPU acceleration [26].

### 3.1 Differentiable Sorting Relaxation

As defined previously, rankings  $\pi$  are lists of indices which are equivalent to permutations of  $\{1, 2, \dots, L\}$ . The set of possible rankings can thus be seen as the symmetric group  $S_L$ , of size  $L!$ . Similarly, every permutation  $\pi$  can be equivalently represented as a permutation matrix  $P_\pi$ , an  $L \times L$  matrix such that its  $(i, \pi_i)$ -th entry is 1 for all  $i \in \{1, 2, \dots, L\}$  and the remaining entries are all 0. The sorting operator is the mapping  $\text{sort} : \mathbb{R}^L \rightarrow S_L$  of a  $L$ -dimensional input vector to the permutation that corresponds to the descending ordering of the vector components. Prior work in relaxing the sorting operator is based on relaxations of either the rankings [18, 26, 27], or the permutation matrices [28–30].

Typically, relaxations to permutation matrices consider the Birkhoff polytope of doubly stochastic matrices. A doubly-stochastic matrix is a square matrix with entries in  $[0, 1]$  where every row and column sum to 1. In contrast, [19] recently proposed an alternate relaxation of permutation matrices, which they refer to as *unimodal* row-stochastic matrix. Such matrices are square matrices with entries in  $[0, 1]$  that require only the entries in every row to sum to 1, but additionally enforce the constraint that the maximizing entry in every row should have a unique column index. See Figure 2 for an example of each type. Note that a unimodal matrix is not necessarily doubly-stochastic and vice versa. Permutation matrices are both doubly-stochastic and unimodal.

In a ranking context, the relaxation of the permutation matrix has the interpretation that the  $i, j$ -th entry denotes the probability of the  $j$ -th element to be ranked at index  $i$ . As seen in Figure 2, the most likely rank assignment of two elements may be the same in the case of a doubly-stochastic relaxation, which is not the case for a unimodal relaxation.

$$\begin{pmatrix} 0 & \mathbf{0.9} & 0.1 \\ \mathbf{0.5} & 0.01 & 0.49 \\ \mathbf{0.5} & 0.09 & 0.41 \end{pmatrix} \quad \begin{pmatrix} \mathbf{0.8} & 0.2 & 0 \\ 0.2 & 0.3 & \mathbf{0.5} \\ 0.25 & \mathbf{0.6} & 0.15 \end{pmatrix}$$

Figure 2: Doubly-stochastic (left) vs. unimodal (right) matrices. Maximum entry in every row in **bold**. Unlike unimodal matrices, two different items can have the same assignment of most-likely ranks (column indices) for doubly-stochastic matrix relaxations.

The latter is thus more appropriate for relaxing LTR objectives based on consistent ranks and will be used in our work.

In general, let  $\hat{P}_{\text{sort}(\mathbf{s})}(\tau)$  denote a relaxation to the permutation matrix  $P_{\text{sort}(\mathbf{s})}$  that can be used for differentiable sorting of an input score vector  $\mathbf{s}$ , for some temperature parameter  $\tau > 0$  such that the true matrix is recovered as  $\tau \rightarrow 0^+$ .

### 3.2 Relaxing Ranking Metrics

We denote by  $f_\theta$  a LTR model (e.g., deep neural network) with parameters  $\theta$  that outputs a vector of  $L$  scores  $\hat{\mathbf{y}} = f_\theta(q, x_1, \dots, x_L)$  for a query  $q$  and  $L$  candidate elements  $\{\mathbf{x}_i\}_{i=1}^L$ . We first consider the NDCG target metric. In Eq. 6, the numerator DCG( $\mathbf{y}, \hat{\pi}$ ) involves computing  $\hat{\pi} = \text{sort}(\hat{\mathbf{y}})$  which is non-differentiable w.r.t.  $\theta$ . Next, we derive a continuous relaxation for DCG( $\mathbf{y}, \hat{\pi}$ ). Let  $\mathbf{g}$  denote the column vector of graded relevance scores such that  $g_j = 2^{y_j} - 1$ . We can then rewrite DCG( $\mathbf{y}, \hat{\pi}$ ) as:

$$\text{DCG}(\mathbf{y}, \hat{\pi}) = \sum_{j=1}^L \frac{g_{\hat{\pi}_j}}{\log_2(1+j)} = \sum_{j=1}^L \frac{[P_{\hat{\pi}} \mathbf{g}]_j}{\log_2(1+j)}. \quad (7)$$

To obtain the DCG@ $k$  objective, one can replace  $L$  with  $k$  in the sum. We omit the suffix @ $k$  in the following, assuming that  $k$  has been defined, potentially equal to  $L$  which would yield the full metric. Since  $\hat{\pi} = \text{sort}(\hat{\mathbf{y}})$ , we can use the relaxation of the permutation matrix to obtain a differentiable relaxation to DCG( $\mathbf{y}, \hat{\pi}$ ) as:

$$\widehat{\text{DCG}}(\mathbf{y}, \hat{\mathbf{y}}, \tau) = \sum_{j=1}^k \frac{[\hat{P}_{\text{sort}(\hat{\mathbf{y}})}(\tau) \mathbf{g}]_j}{\log_2(1+j)}. \quad (8)$$

Substituting this in the expression for NDCG in Eq. 6, we obtain the following relaxation for NDCG:

$$\widehat{\text{NDCG}}(\mathbf{y}, \hat{\mathbf{y}}, \tau) = \frac{\widehat{\text{DCG}}(\mathbf{y}, \hat{\mathbf{y}}, \tau)}{\text{DCG}(\mathbf{y}, \pi^*)} \quad (9)$$

where the normalization in the denominator does not depend on  $\theta$  and can be computed exactly via regular sorting. Finally, we define the PiRank surrogate loss for NDCG as follows:

$$\ell_{\text{PiRank-NDCG}} = 1 - \widehat{\text{NDCG}}(\mathbf{y}, \hat{\mathbf{y}}, \tau) \quad (10)$$

which is bounded between 0 and 1 as is NDCG, and whose difference with the actual  $(1 - \text{NDCG})$  gets negligible as  $\tau \rightarrow 0^+$ . Figure 3 illustrates the model architecture for the above objective. Similarly, we can derive a surrogate loss for the ARP metric in Eq. 4 as:

$$\hat{\ell}_{\text{PiRank-ARP}}(\mathbf{y}, \hat{\mathbf{y}}, \tau) = \frac{\sum_{j=1}^k [\hat{P}_{\text{sort}(\hat{\mathbf{y}})}(\tau) \mathbf{y}]_j j}{\sum_{j=1}^k y_j}. \quad (11)$$

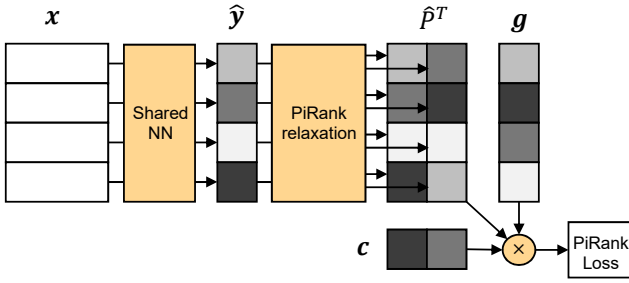


Figure 3: Architecture for the computation of the PiRank relaxed NDCG@k loss for  $L = 4$  and  $k = 2$ . Square cells represent scalars with darker shades indicating higher values. The fourth item has currently the highest score as given by the neural network but the second item has the highest relevance. The vector  $c$ , with components  $c_j = 1/\log(1 + j)$ , discounts gains  $g$  based on rankings.

### 3.3 Differentiable Top- $k$ Ranking Relaxation

Our PiRank losses only require the first  $k$  rows of the relaxed permutation matrix  $\hat{P}_{\text{sort}}(\hat{\mathbf{y}})$ . This is specific to the LTR setting in which only the top-ranked items are of interest, in contrast to the full sorting problem that requires the full matrix.

In NeuralSort [19], a unimodal relaxation  $\hat{P}_{\text{sort}}(\hat{\mathbf{y}})(\tau)$  can be defined as follows. Let  $A_{\hat{\mathbf{y}}}$  denote the matrix of absolute pairwise differences with  $i, j$ -th entry given as  $[A_{\hat{\mathbf{y}}}]_{ij} = |\hat{y}_i - \hat{y}_j|$ . Then, the  $i$ -th row of the relaxed permutation matrix is:

$$\hat{P}_{\text{sort}}^{(NS)}(\hat{\mathbf{y}})(\tau)_{i,\cdot} = \text{softmax}[(n+1-2i)\hat{\mathbf{y}} - A_{\hat{\mathbf{y}}}\mathbb{1}]/\tau \quad (12)$$

where  $\mathbb{1}$  is the vector with all components equal to 1. This unimodal relaxation is particularly well-suited to extracting top- $k$  items. However, the complexity to obtain the top- $k$  rows in this formulation, even for  $k$  as low as 1, is quadratic in  $L$  as the full computation of  $A_{\hat{\mathbf{y}}}\mathbb{1}$  is required for the softmax operation in Eq. 12. This is prohibitive when  $L \gg k$ , a common scenario, and motivates the introduction of a new top- $k$  ranking relaxation with more favorable complexity.

The proposed process can be seen as a relaxed and truncated multi-way merge sort algorithm. Let  $L = b_1 b_2 \dots b_d$  be a factorization of the list size  $L$  into  $d$  positive integers. The scores  $\hat{\mathbf{y}}$  can then be split in size-1 vectors and set as the values of the leaves of a tree of depth  $d$  with branching factor  $b_j$  at height  $j$ . Let  $\{k_j\}_{j=0}^d$  be sizes for the intermediate results during the merge process, such that  $k_0 = 1$  and  $\min(k, k_{j-1}b_j) \leq k_j \leq k_{j-1}b_j$  for  $j \geq 1$  (explained below). Then, in an iterative manner for  $j = 1, \dots, d$ , a node at height  $j$  takes as value the top- $k_j$  scores given by the application of the NeuralSort operator on the concatenation of the values of its children. With  $k_d = k$ , the root value thus obtained is a relaxation of the top- $k$  scores in  $\hat{\mathbf{y}}$ . See Figure 4 for an example. The top- $k$  rows of the relaxed permutation matrix  $\hat{P}_{\text{sort}}(\hat{\mathbf{y}})$  yielding these scores are constructed by compounding the operations at each iteration.

The intuition behind the favorable scaling is as follows. At step  $j$ , NeuralSort is applied on blocks of size  $k_{j-1}b_j$  due to merging  $b_j$  sub-blocks of size  $k_{j-1}$ . Obtaining the full sorted list of scores would require to keep all intermediate scores during the process, meaning  $k_j^{(\max)} = b_1 \dots b_j = k_{j-1}b_j$  for

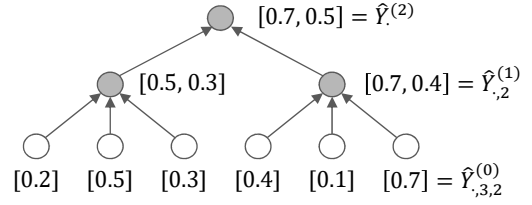


Figure 4: Tree representation of the algorithm in the case  $L = 6 = 3 \cdot 2$ ,  $k = 2$  and  $\hat{\mathbf{y}}^T = (0.2, 0.5, 0.3, 0.4, 0.1, 0.7)$ . The scores are merged in groups of  $b_1 = 3$  and the respective top  $k_1 = 2$  scores are kept, then the  $b_2 = 2$  outputs are merged and the final top  $k_2 = k = 2$  scores are obtained. The effect of relaxation is not shown for readability. At non-zero temperature, the values at non-terminal nodes would be linear combination of the scores.

$j \geq 1$ . In the last step, the NeuralSort operator is applied on a list of size  $k_{d-1}b_d$ , equal to  $L$  in this case, so the overall complexity would be at least quadratic in  $L$  as explained previously. However, since only the top- $k$  scores are desired, intermediate outputs can be truncated if larger than  $k$ . Full truncation corresponds to  $k_j^{(\min)} = \min(k, k_{j-1}b_j)$ . Any choice  $k_j^{(\min)} \leq k_j \leq k_j^{(\max)}$  is acceptable to recover the top- $k$  scores, with larger values allowing more information to flow at the expense of a higher complexity. Choosing  $b_j \approx L^{1/d}$  and  $k_j$  minimal, the list sizes  $b_j k_{j-1}$  on which NeuralSort is applied at each step can thus be of the order of  $L^{1/d}k$ , much smaller than  $L$  in the  $d > 1$  and  $k \ll L$  scenario.

Formally, let  $b_j$  and  $k_j$  for  $j \in \{1, \dots, d\}$  defined and constrained as in the previous paragraphs. Additionally, let  $\tau_1, \tau_2, \dots, \tau_d$  be the relaxation temperatures at each height, with  $\tau_d = \tau$  and  $\tau_j \leq \tau_{j+1}$  for  $j \in \{1, \dots, d-1\}$ . Define the tensor  $\hat{\mathbf{Y}}^{(0)}$  by reshaping  $\hat{\mathbf{y}}$  to shape  $(k_0, b_1, b_2, \dots, b_d)$ , yielding components

$$\hat{\mathbf{Y}}_{1,i_1,i_2,\dots,i_d}^{(0)} = \hat{y}_{1+\sum_{j=1}^d(i_j-1)\prod_{l=1}^{j-1}b_l}, \quad (13)$$

with  $i_j \in \{1, \dots, b_j\}$  and the first index is always 1 as  $k_0 = 1$ . With the tree representation, the first tensor index is the position in the node value vector and the rest of the indices identify the node by the index of each branching from the root. For  $j \in \{1, 2, \dots, d\}$ , recursively define the tensors  $\hat{\mathbf{Q}}^{(j)}$ ,  $\hat{\mathbf{Y}}^{(j)}$  and  $\hat{\mathbf{P}}^{(j)}$  of respective shapes  $(k_j, k_{j-1}, b_j, \dots, b_d)$ ,  $(k_j, b_{j+1}, \dots, b_d)$  and  $(k_j, b_1, \dots, b_d)$  with components

$$\begin{aligned} \hat{\mathbf{Q}}_{l,m,i_j,\dots,i_d}^{(j)} &= \text{softmax} \left[ \left( (k_{j-1}b_j + 1 - 2l)\hat{\mathbf{Y}}_{m,i_j,\dots,i_d}^{(j-1)} \right. \right. \\ &\quad \left. \left. - \sum_{p=1}^{k_{j-1}} \sum_{q=1}^{b_j} \left| \hat{\mathbf{Y}}_{m,i_j,i_{j+1},\dots,i_d}^{(j-1)} - \hat{\mathbf{Y}}_{p,q,i_{j+1},\dots,i_d}^{(j-1)} \right| \right) / \tau_j \right] \\ \hat{\mathbf{Y}}_{l,i_{j+1},\dots,i_d}^{(j)} &= \sum_{p=1}^{k_{j-1}} \sum_{q=1}^{b_j} \hat{\mathbf{Q}}_{l,p,q,i_{j+1},\dots,i_d}^{(j)} \hat{\mathbf{Y}}_{p,q,i_{j+1},\dots,i_d}^{(j-1)} \\ \hat{\mathbf{P}}_{l,i_1,\dots,i_d}^{(j)} &= \sum_{m=1}^{k_{j-1}} \hat{\mathbf{Q}}_{l,m,i_j,\dots,i_d}^{(j)} \hat{\mathbf{P}}_{m,i_1,i_2,\dots,i_d}^{(j-1)}, \end{aligned} \quad (14)$$

with  $\hat{P}^{(0)} = 1$ . Intuitively,  $\hat{Y}^{(j)}$  holds the relaxed top- $k_j$  scores at height  $j$  and  $\hat{Y}^{(d)}$  is the desired top- $k$  score vector. The interpretation of the indices in the tree structure is as for  $\hat{Y}^{(0)}$ , illustrated in Figure 4. More importantly, we keep track of the relaxed sorting operation that yielded this output.  $\hat{Q}^{(j)}$  is the relaxed permutation matrix obtained by applying the NeuralSort operator in Eq. 12 to  $\hat{Y}^{(j)}$ , while  $\hat{P}^{(j)}$  compounds the relaxed permutation matrices obtained so far so it always maps from the initial list size. Finally, define the  $k \times L$  matrix  $\hat{P}$  by reshaping the tensor  $P^{(d)}$ , yielding components

$$\hat{P}_{l, 1 + \sum_{j=1}^d (i_j - 1) \prod_{l=1}^{j-1} b_l} = \hat{P}_{l, i_1, \dots, i_d}^{(d)} \quad (15)$$

for  $i_j \in \{1, \dots, b_j\}$ . The  $k$  rows of  $\hat{P}$  are used as the top- $k$  rows of the relaxed sorting operator  $\hat{P}_{\text{sort}(\hat{y})}(\tau)$ . This approach is equivalent to NeuralSort, yielding Eq. 12 for  $d = 1$ . Proof of convergence for  $\tau \rightarrow 0^+$  of this relaxation in the general case  $d \geq 1$  is presented in Appendix B

In the simple case where  $L = b^d$  and we set  $b_j = b$ ,  $k_j = \min(k, b^j)$  for all  $j \in \{1, \dots, d\}$ , the complexity to compute  $\hat{P}$  and thus the PiRank losses is then  $O(L^{1+1/d} + (d-1)k^2L)$ , which scales favorably in  $L$  if  $d > 1$  and  $k = O(1)$ .

## 4 Experiments

We present two sets of experiments in this section: (a) benchmark evaluation comparing PiRank with other ranking based approaches on available large-scale benchmark LTR datasets, and (b) ablation experiments for the design choices in PiRank.

### 4.1 Benchmark Evaluation via TF-Ranking

**Datasets.** To empirically test PiRank, we consider two of the largest open-source benchmarks for LTR: the MSLR-WEB30K<sup>2</sup> and the Yahoo! LTR dataset C14<sup>3</sup>. Both datasets have relevance scores on a 5-point scale of 0 to 4, with 0 denoting complete irrelevance and 4 denoting perfect relevance. We give extensive details on the datasets and experimental protocol in Appendix C for reproducibility.

**Baselines.** We focus on neural network-based approaches and use the open-source TensorFlow Ranking (TFR) framework [21]. TFR consists of high-quality GPU-friendly implementations of several LTR approaches, common evaluation metrics, and standard data loading formats. We compare our approach, PiRank, with the following baselines provided by TensorFlow Ranking: Approximate NDCG Loss [25], Pairwise Logistic Loss (RankNet), Pairwise Logistic Loss with lambda-NDCG weights (LambdaRank), and the Softmax Loss. Of these methods, only the Pairwise Logistic Loss (RankNet) is a fully pairwise approach. We also include NeuralSort, whose loss is the cross-entropy of the predicted permutation matrix. We omit tree-based methods such as LambdaMART [31] to focus on methods that can learn end-to-end from unstructured data and leverage GPU acceleration.

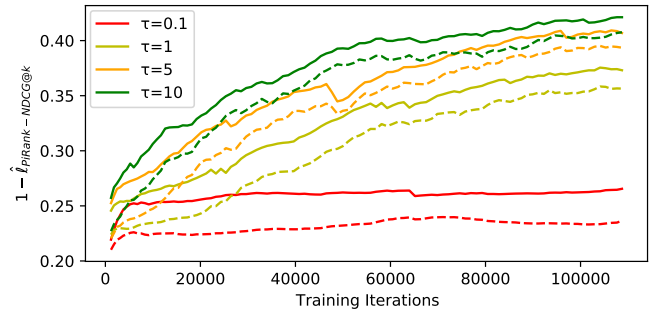


Figure 5:  $1 - \hat{\ell}_{\text{PiRank-NDCG@k}}$  ( $k = 10$ , full lines) for different values of the temperature parameter  $\tau$ , with the corresponding value of the hard metric NDCG@10 (dashed lines), at validation.

**Settings.** All approaches use the same 6-layer fully connected network architecture with ReLU activations to compute the scores  $\hat{y}$  for all (query, item) pairs, trained on 100 epochs. The list size for each group of items to score and rank is fixed to 100, for both training and testing. Further experimental details are deferred to Appendix C.

**Metrics.** We evaluate Ordered Pair Accuracy (OPA), Average Relevance Position (ARP), Mean Reciprocal Rank (MRR), and NDCG@ $k$  with  $k \in \{1, 3, 5, 10, 15, 100\}$ .

**Results.** Our results are shown in Table 1. Overall, PiRank shows similar or better performance than baselines on all metrics. On MSLR-WEB30K, PiRank outperforms baselines across all metrics. On average, for this dataset, we notice a 8.27% increase across metrics (12.3% for NDCG's), with performance being noticeably better on NDCG with a smaller cutoff  $k$  (27.3% for NDCG@1), as shown in Figure 6. This suggests that our approach might be particularly suited to rank top items, whose appropriate placement has more impact on NDCG@ $k$  with small  $k$ . As  $k$  increases, pairwise methods such as RankNet that do not perform well on large lists start to perform similarly to PiRank and other listwise baselines, as a larger value of  $k$  is more forgiving. On Yahoo! C14, PiRank is the best performing approach on NDCG@ $k$  when  $k \geq 3$ , but the metric-independent NeuralSort performs better on non-NDCG metrics.

### 4.2 Ablation Experiments

**Temperature.** The temperature hyperparameter  $\tau$  is used in PiRank to control the degree of relaxation. We experiment on several values ( $\tau \in \{0.1, 1, 5, 10\}$ ) using the same settings as in Section 4.1, on the MSLR-WEB30K dataset. Figure 5 demonstrates the importance of correctly tuning  $\tau$ . High values ( $\tau > 1$ ) speed up training, especially in the early regime, while low values induce large gradient norms which are unsuitable for training and lead to the loss stalling or even diverging. Another observation is that the relaxed metric  $1 - \hat{\ell}_{\text{PiRank-NDCG@k}}$  closely follows the value of the downstream metric NDCG@ $k$  as expected.

**Training List Size.** The training list size parameter  $L_{\text{train}}$  determines the number of items to rank for a query during training. We train PiRank in the same setting as Section 4.1, but with training list sizes  $L_{\text{train}} \in \{10, 20, 40, 100\}$  which

<sup>2</sup><https://www.microsoft.com/en-us/research/project/mslr/>

<sup>3</sup><https://webscope.sandbox.yahoo.com>



	Loss / Metric	OPA	ARP	MRR	NDCG@1	NDCG@3	NDCG@5	NDCG@10	NDCG@15	NDCG@100
(a)	Pairwise Logistic	0.5712	43.0730	0.6718	0.2241	0.2587	0.2823	0.3205	0.3489	0.6253
	PL (Lambda)	0.5797	42.8132	0.7284	0.2882	0.3062	0.3240	0.3579	0.3840	0.6461
	Softmax	0.5475	44.7017	0.6796	0.2165	0.2395	0.2598	0.2993	0.3279	0.6131
	Approx. NDCG	0.5548	44.5704	0.7279	0.2682	0.2814	0.2940	0.3203	0.3429	0.6243
	NeuralSort	0.5331	45.7840	0.6269	0.1666	0.1942	0.2184	0.2591	0.2873	0.5875
	PiRank-NDCG	<b>0.5876</b>	<b>42.2811</b>	<b>0.7776</b>	<b>0.3668</b>	<b>0.3576</b>	<b>0.3656</b>	<b>0.3873</b>	<b>0.4078</b>	<b>0.6634</b>

	Loss / Metric	OPA	ARP	MRR	NDCG@1	NDCG@3	NDCG@5	NDCG@10	NDCG@15	NDCG@100
(b)	Pairwise Logistic	0.6885	15.9540	0.8973	0.6577	0.6701	0.6971	0.7496	0.7772	0.8423
	PL (Lambda)	0.6754	16.1032	0.8940	0.6558	0.6703	0.6956	0.7473	0.7746	0.8415
	Softmax Loss	0.6955	15.8613	0.8991	0.6635	0.6805	0.7065	0.7568	0.7840	0.8476
	Approx. NDCG	0.6827	16.0131	0.9036	<b>0.6946</b>	0.6925	0.7153	0.7620	0.7882	0.8531
	NeuralSort	<b>0.6961</b>	<b>15.8547</b>	<b>0.9071</b>	0.6831	0.6899	0.7134	0.7619	0.7888	0.8521
	PiRank-NDCG	0.6816	16.0142	0.9039	0.6920	<b>0.6967</b>	<b>0.7174</b>	<b>0.7650</b>	<b>0.7900</b>	<b>0.8540</b>

Table 1: Benchmark evaluation on (a) MSLR-WEB30K and (b) Yahoo! C14 test sets.

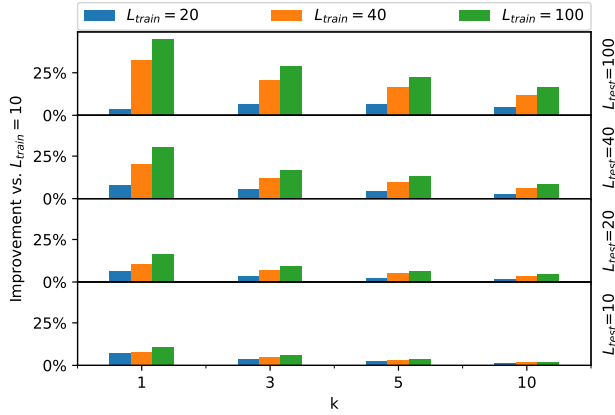


Figure 6: Relative improvement of NDCG@k on different values of  $L_{test}$ , for different  $L_{train}$  values vs. a baseline of  $L_{train} = 10$ .

we then evaluate on testing list sizes in the same range of values  $L_{test} \in \{10, 20, 40, 100\}$ . The dataset is again MSLR-WEB30K. Figure 6 exposes four patterns for NDCG@k. First, for a fixed  $L_{test}$  and  $k$ , a larger  $L_{train}$  is always better. Second, for a fixed  $L_{test}$ , we observe diminishing returns along  $k$ , as relative improvements decrease for all  $L_{train}$ . This observation is confounded by NDCG@k values growing larger with  $k$ , but the metric is always able to distinguish between ranking functions [32]. Third, for a fixed  $k$ , our returns along  $L_{test}$  increase with  $L_{train}$  (except for  $L_{train} = 20$  and  $k = 1$ ). This means that the need for a larger  $L_{train}$  is more pronounced for larger values of  $L_{test}$ . Fourth and last, the returns increase most dramatically with  $L_{train}$  when  $L_{test} \gg k$  (top left), a common industrial setting. Values for NDCG@k, MRR, OPA, ARP are provided in Appendix D. For MRR, using a larger  $L_{train}$  is always beneficial regardless of  $L_{test}$ , but not always for OPA and ARP.

**Depth.** A main advantage of the PiRank approach is how it can scale to very large training list sizes  $L_{train}$ . This setting is difficult to come across with traditional LTR datasets, which are manually annotated, but occurs frequently in practice. One example is when the relevance labels are obtained from implicit signals such as clicks or purchases in recommendation systems. In this case, an LTR model is used to re-rank a list of candidates generated by another, simpler,

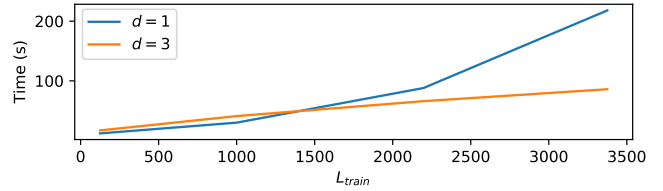


Figure 7: Wall-clock time for 100 training steps, each corresponding to 16 queries, for different  $L_{train}$  and maximal depth  $d$ . This shows the effect on complexity as  $d$  increases. We use  $k = 1$  and  $L_{train} = 5^3, 10^3, 13^3$  and  $15^3$  such that  $L_{train} = b^3$  for  $d = 3$  and  $k_j = 1$ .

model choosing among all possible items those potentially relevant to a query or context. An LTR model capable of handling very large lists can reduce the impact of errors made by the simpler candidate generation step, moving to the top an item lowly ranked at first that would have been cut off from a smaller list. To test the complexity shown in Section 3.3 in extreme conditions, we create a synthetic dataset as described in Appendix E. Figure 7 shows how the training time for depth  $d = 3$  scales much more favorably than for  $d = 1$ , following their respective time complexities of  $O(L^{1+1/3})$  and  $O(L^2)$ .

## 5 Conclusion

In this work, we have introduced PiRank, a novel approach to designing surrogate loss functions for Learning-To-Rank (LTR) that leverages a continuous, temperature-controlled unimodal relaxation to the sorting operator [19] as a building block and can scale to very large lists. This allows us to recover exact expressions of the commonly used non-differentiable ranking metrics in the limit of zero temperature, which we proved in particular for the NDCG metric. In our experiments on the largest publicly available LTR datasets, we observed that PiRank outperforms competing methods on the MSLR-WEB30K and Yahoo! C14 benchmarks on 14/18 ranking metrics and their variants. We also confirmed that our approach scales favorably to large datasets.

## 6 ACKNOWLEDGEMENTS

Stefano Ermon is supported in part from NSF (#1651565, #1522054, #1733686), ONR (N00014-19-1-2145), AFOSR (FA9550-19-1-0024) and Bloomberg.

## References

- [1] Tie-Yan Liu et al. Learning to rank for information retrieval. *Foundations and Trends® in Information Retrieval*, 3(3):225–331, 2009.
- [2] David Cossock and Tong Zhang. Subset ranking using regression. In *International Conference on Computational Learning Theory*, pages 605–619. Springer, 2006.
- [3] Ping Li, Qiang Wu, and Christopher J Burges. Mcrank: Learning to rank using multiple classification and gradient boosting. In *NeurIPS*, pages 897–904, 2008.
- [4] Koby Crammer and Yoram Singer. Pranking with ranking. In *NeurIPS*, pages 641–647, 2002.
- [5] Amnon Shashua and Anat Levin. Ranking with large margin principle: Two approaches. In *NeurIPS*, pages 961–968, 2003.
- [6] Ralf Herbrich. Large margin rank boundaries for ordinal regression. *Advances in large margin classifiers*, pages 115–132, 2000.
- [7] Yoav Freund, Raj Iyer, Robert E Schapire, and Yoram Singer. An efficient boosting algorithm for combining preferences. *JMLR*, 4(Nov):933–969, 2003.
- [8] Chris Burges, Tal Shaked, Erin Renshaw, Ari Lazier, Matt Deeds, Nicole Hamilton, and Greg Hullender. Learning to rank using gradient descent. *ICML ’05*, pages 89–96, 2005.
- [9] Christopher JC Burges. From ranknet to lambdarank to lambdamart: An overview. *Learning*, 11(23-581):81, 2010.
- [10] Zhaohui Zheng, Hongyuan Zha, Tong Zhang, Olivier Chapelle, Keke Chen, and Gordon Sun. A general boosting method and its application to learning ranking functions for web search. In *NeurIPS*, pages 1697–1704, 2008.
- [11] Yunbo Cao, Jun Xu, Tie-Yan Liu, Hang Li, Yalou Huang, and Hsiao-Wuen Hon. Adapting ranking svm to document retrieval. In *SIGIR*, pages 186–193. ACM, 2006.
- [12] Christopher J.C. Burges, Robert Ragno, and Quoc Viet Le. Learning to rank with nonsmooth cost functions. *Advances in Neural Information Processing Systems*, pages 193–200, 2007.
- [13] Mingrui Wu, Yi Chang, Zhaohui Zheng, and Hongyuan Zha. Smoothing dcg for learning to rank: A novel approach using smoothed hinge functions. In *CIKM*, pages 1923–1926. ACM, 2009.
- [14] Zhe Cao, Tao Qin, Tie-Yan Liu, Ming-Feng Tsai, and Hang Li. Learning to rank: from pairwise approach to listwise approach. In *ICML*, pages 129–136. ACM, 2007.
- [15] Fen Xia, Tie-Yan Liu, Jue Wang, Wensheng Zhang, and Hang Li. Listwise approach to learning to rank: theory and algorithm. In *ICML*, pages 1192–1199. ACM, 2008.
- [16] Jun Xu and Hang Li. Adarank: a boosting algorithm for information retrieval. In *SIGIR*, pages 391–398. ACM, 2007.
- [17] Yisong Yue, Thomas Finley, Filip Radlinski, and Thorsten Joachims. A support vector method for optimizing average precision. In *SIGIT*, pages 271–278. ACM, 2007.
- [18] Michael Taylor, John Guiver, Stephen Robertson, and Tom Minka. Softrank: optimizing non-smooth rank metrics. In *WSDM*, pages 77–86. ACM, 2008.
- [19] Aditya Grover, Eric Wang, Aaron Zweig, and Stefano Ermon. Stochastic optimization of sorting networks via continuous relaxations. In *ICLR*, 2019.
- [20] Tao Qin and Tie-Yan Liu. Introducing LETOR 4.0 Datasets. 2013.
- [21] Rama Kumar Pasumarthi, Sebastian Bruch, Xuanhui Wang, Cheng Li, Michael Bendersky, Marc Najork, Jan Pfeifer, Nadav Golbandi, Rohan Anil, and Stephan Wolf. Tf-ranking: Scalable tensorflow library for learning-to-rank. In *ACM SIGKDD*, pages 2970–2978. ACM, 2019.
- [22] Tie-Yan Liu. *Learning to rank for information retrieval*. Springer Science & Business Media, 2011.
- [23] Mu Zhu. Recall, precision and average precision. *Department of Statistics and Actuarial Science, University of Waterloo, Waterloo*, 2:30, 2004.
- [24] Kalervo Järvelin and Jaana Kekäläinen. Cumulated gain-based evaluation of ir techniques. *ACM Transactions on Information Systems (TOIS)*, 20(4):422–446, 2002.
- [25] Tao Qin, Tie-Yan Liu, and Hang Li. A general approximation framework for direct optimization of information retrieval measures. *Information retrieval*, 13(4):375–397, 2010.
- [26] Mathieu Blondel, Olivier Teboul, Quentin Berthet, and Josip Djolonga. Fast differentiable sorting and ranking. In *proceedings of ICML 2020 arXiv:2002.08871*, 2020.
- [27] Olivier Chapelle and Mingrui Wu. Gradient descent optimization of smoothed information retrieval metrics. *Information retrieval*, 13(3):216–235, 2010.
- [28] Ryan Prescott Adams and Richard S Zemel. Ranking via sinkhorn propagation. *arXiv preprint arXiv:1106.1925*, 2011.
- [29] Gonzalo Mena, David Belanger, Scott Linderman, and Jasper Snoek. Learning Latent Permutations with Gumbel-Sinkhorn Networks. In *ICLR*, 2018.
- [30] Marco Cuturi, Olivier Teboul, and Jean-Philippe Vert. Differentiable Ranks and Sorting using Optimal Transport. (NeurIPS), 2019.
- [31] Chris Burges. From RankNet to LambdaRank to LambdaMART: An Overview. *JMLR*, 41(4):574–581, 2010.
- [32] Yining Wang, Liwei Wang, Yuanzhi Li, Di He, Wei Chen, and Tie Yan Liu. A theoretical analysis of NDCG ranking measures. *JMLR*, 30:25–54, 2013.
- [33] Leonardo Rigutini, Tiziano Papini, Marco Maggini, and Franco Scarselli. Sortnet: Learning to rank by a neural preference function. *IEEE transactions on neural networks*, 22(9):1368–1380, 2011.
- [34] Ziqiang Cao, Furu Wei, Li Dong, Sujian Li, and Ming Zhou. Ranking with recursive neural networks and its application to multi-document summarization. *AAAI*, pages 2153–2159, 2015.
- [35] Chenyan Xiong, Zhuyun Dai, Jamie Callan, Zhiyuan Liu, and Russell Power. End-to-end neural ad-hoc ranking with kernel pooling. In *ACM SIGIR*, pages 55–64. ACM, 2017.
- [36] Robin L Plackett. The analysis of permutations. *Applied Statistics*, pages 193–202, 1975.
- [37] R Duncan Luce. *Individual choice behavior: A theoretical analysis*. Courier Corporation, 1959.
- [38] Yoshua Bengio, Nicholas Léonard, and Aaron Courville. Estimating or propagating gradients through stochastic neurons for conditional computation. *arXiv preprint arXiv:1308.3432*, 2013.
- [39] O. Tange. Gnu parallel - the command-line power tool. *login: The USENIX Magazine*, 36(1):42–47, Feb 2011.

## Appendices

### A Further Related Works

**Pairwise approaches.** Closely related to RankNet, pairwise approaches such as Sortnet [33] and SmoothRank [27] casts sorting of  $n$  elements as performing  $n^2$  pairwise comparisons, and try to approximate the pairwise comparison operator for sorting. We consider a more direct relaxation with attractive properties for rankings that we describe in Section 3.

**Listwise approaches.** include ListNet [34] and ListMLE [35], which define surrogate losses that take into consideration the full predicted rank ordering while being agnostic to the downstream ranking metrics. ListNet for instance considers the predicted scores as parameters for the Plackett-Luce distribution [36, 37] and learns these scores via maximum likelihood estimation.

### B Proof of Convergence

Used in a PiRank surrogate loss of Section 3.2, the relaxation presented in Section 3.3 recovers the downstream metric by lowering the temperature as formalized in the result below for NDCG.

**Proposition 1.** *If we assume that the entries of  $\hat{\mathbf{y}}$  are drawn independently from a distribution that is absolutely continuous w.r.t. the Lebesgue measure in  $\mathbb{R}$ , then the following convergence holds almost surely:*

$$\lim_{\tau \rightarrow 0^+} \hat{\ell}_{\text{PiRank-NDCG}}(\mathbf{y}, \hat{\mathbf{y}}, \tau) = 1 - \text{NDCG}(\mathbf{y}, \hat{\pi}) \quad (16)$$

where  $\hat{\pi} = \text{sort}(\hat{\mathbf{y}})$ .

*Proof.* In the  $d > 1$  case, the limit is interpreted as

$$\lim_{\tau \rightarrow 0^+} = \lim_{\tau_d \rightarrow 0^+} \lim_{\tau_{d-1} \rightarrow 0^+} \dots \lim_{\tau_1 \rightarrow 0^+} \quad (17)$$

given the increasing ordering of the temperatures by height and the constraint  $\tau_d = \tau$ .

We first sketch a proof by induction on the height  $j$  that, under the same assumptions as the proposition, for all  $i_{j+1}, \dots, i_d$ , the  $k'_j$ -dimensional vector

$$\mathbf{y}_{i_{j+1}, \dots, i_d}^{(j)} \equiv \lim_{\tau_j \rightarrow 0^+} \hat{\mathbf{Y}}_{:k'_j, i_{j+1}, \dots, i_d}^{(j)} \quad (18)$$

with  $k'_j = \min(k, k_j)$  and  $:l$  the top- $l$  rows extraction, contains the top- $k'_j$  scores in  $\hat{\mathbf{Y}}_{:, \dots, i_{j+1}, \dots, i_d}^{(0)}$  in descending order and the  $k'_j \times L_j$  matrix

$$P_{i_{j+1}, \dots, i_d}^{(j)} \equiv \lim_{\tau_j \rightarrow 0^+} \hat{P}_{:k'_j, i_{j+1}, \dots, i_d}^{(j)} \quad (19)$$

with  $L_j = b_1 \dots b_j$  is the row-truncated permutation matrix realizing the ordering,

$$\mathbf{y}_{i_{j+1}, \dots, i_d}^{(j)} = P_{i_{j+1}, \dots, i_d}^{(j)} \hat{\mathbf{Y}}_{:, \dots, i_{j+1}, \dots, i_d}^{(0)} \quad (20)$$

where reshaping as necessary is implicit in the above two equations.

Table 2: Shared experiment parameters

Parameter	Value
Hidden layer sizes	256, 256, 128, 128, 64, 64
Hidden layer activations	ReLU
Batch size	16
Training list size	100
Testing list size	100
Learning rate	1.00E-05
Number of epochs	100
Optimizer	Adam

For  $j = 0$ , this is trivial as  $P^{(0)} = 1$  and by convention  $b_0 = k_0 = 1$ .

Assuming the above is true for a height  $j - 1$ , the top- $k'_j$  scores in  $\hat{\mathbf{Y}}_{:, \dots, i_{j+1}, \dots, i_d}^{(0)}$  are included in the concatenation of the vectors  $\hat{\mathbf{Y}}_{:, i_j, \dots, i_d}^{(j-1)}$  for  $i_j \in \{1, \dots, b_j\}$  in the  $\tau_{j-1} \rightarrow 0^+$  limit from the assumption (no limit for  $j = 1$ ).  $\hat{\mathbf{Q}}_{:, \dots, i_{j+1}, \dots, i_d}^{(j)}$  is then the NeuralSort relaxed permutation matrix for these concatenated vector. From Theorem 1 of [19], we know that in the  $\tau_j \rightarrow 0^+$  limit, this matrix will converge to the sorting permutation matrix. In this limit,  $\hat{\mathbf{Y}}_{:, i_{j+1}, \dots, i_d}^{(j)}$  is then sorted version of the concatenated vector, so that in particular its top- $k'_j$  elements are the sorted top- $k'_j$  elements of the concatenated vector, proving the claim on  $\mathbf{y}_{i_{j+1}, \dots, i_d}^{(j)}$ . Further, the claim on  $P^{(j)}$  directly derives from the previous observation on the limit of  $\hat{\mathbf{Q}}_{:, \dots, i_{j+1}, \dots, i_d}^{(j)}$  and the fact that a product of permutation matrices which is the matrix of the product of the permutations. This finishes the proof by induction.

Taking  $j = d$ , we obtain from Eq. 20 and the nature of permutation matrices that

$$\lim_{\tau \rightarrow 0^+} \hat{P}_{\text{sort}(\hat{\mathbf{y}})}(\tau)_{:k} = [P_{\text{sort}(\hat{\mathbf{y}})}]_{:k}. \quad (21)$$

From limit calculus, we know that the limit of finite sums is the sum of the limits and hence, substituting the above result in Eq. 8 we have:

$$\lim_{\tau \rightarrow 0^+} \widehat{\text{DCG}}(\mathbf{y}, \hat{\mathbf{y}}, \tau) = \text{DCG}(\mathbf{y}, \hat{\pi}). \quad (22)$$

Substituting the above in Eq. 9 and Eq. 10 proves the proposition.  $\square$

Note that the assumption of independent draws is needed to ensure that the elements of  $\hat{\mathbf{y}}$  are distinct almost surely.

### C Experimental Details

**Datasets.** We test PiRank on MSLR-WEB30K<sup>4</sup> and the Yahoo! LTR dataset C14<sup>5</sup>. MSLR-WEB30K contains 30,000 queries from Bing with feature vectors of length 136, while Yahoo! C14 dataset comprises 36,000 queries, 883,000 items

<sup>4</sup><https://www.microsoft.com/en-us/research/project/mslr/>

<sup>5</sup><https://webscope.sandbox.yahoo.com>



Table 3: Training list size effectiveness on ranking metrics

OPA	$L_{train}$			
$L_{test}$	10	20	40	100
10	0.5830	0.5947	0.5939	<b>0.5949</b>
20	0.5852	0.5949	<b>0.5961</b>	0.5926
40	0.5816	0.5935	<b>0.5942</b>	0.5915
100	0.5755	0.5859	<b>0.5867</b>	0.5844
MRR	$L_{train}$			
$L_{test}$	10	20	40	100
10	0.6691	0.6830	0.6912	<b>0.6949</b>
20	0.6835	0.7048	0.7087	<b>0.7172</b>
40	0.6732	0.7042	0.7230	<b>0.7350</b>
100	0.6628	0.6985	0.7301	<b>0.7548</b>
ARP	$L_{train}$			
$L_{test}$	10	20	40	100
10	5.0164	4.9584	4.9662	<b>4.9428</b>
20	9.4277	9.3431	<b>9.3334</b>	9.3401
40	18.3042	18.0688	<b>18.0493</b>	18.0617
100	42.9107	42.4183	<b>42.3972</b>	42.4091
NDCG@1	$L_{train}$			
$L_{test}$	10	20	40	100
10	0.3850	0.4127	0.4140	<b>0.4261</b>
20	0.3320	0.3521	0.3670	<b>0.3860</b>
40	0.2829	0.3054	0.3403	<b>0.3683</b>
100	0.2569	0.2665	0.3401	<b>0.3713</b>
NDCG@3	$L_{train}$			
$L_{test}$	10	20	40	100
10	0.4610	0.4793	0.4826	<b>0.4878</b>
20	0.3757	0.3885	0.4017	<b>0.4092</b>
40	0.3188	0.3373	0.3572	<b>0.3731</b>
100	0.2780	0.2963	0.3349	<b>0.3579</b>
NDCG@5	$L_{train}$			
$L_{test}$	10	20	40	100
10	0.5358	0.5498	0.5531	<b>0.5570</b>
20	0.4181	0.4271	0.4388	<b>0.4441</b>
40	0.3447	0.3607	0.3780	<b>0.3896</b>
100	0.2971	0.3158	0.3461	<b>0.3635</b>
NDCG@10	$L_{train}$			
$L_{test}$	10	20	40	100
10	0.6994	0.7100	0.7115	<b>0.7141</b>
20	0.5090	0.5165	0.5257	<b>0.5305</b>
40	0.3989	0.4106	0.4243	<b>0.4337</b>
100	0.3330	0.3485	0.3720	<b>0.3878</b>

and feature vectors of length 700. In both datasets, the number of items per query can exceed 100, or even 1,000 in the case of MSLR-WEB30K. Both datasets have relevance scores on a 5-point scale of 0 to 4, with 0 denoting complete irrelevance and 4 denoting perfect relevance. Note that when using binary classification-based metrics such as mean-reciprocal rank, ordinal relevance score from 1 to 4 are mapped to ones. MSLR-WEB30K is provided in folds of training / validation / test sets rotating on 5 subsets of data, and we choose to use Fold1 for our experiments. For Yahoo! C14, we use “Set 1” which is the larger of the two provided sets. For both datasets, we use the standard train/validation/test splits. We use the validation split for both early stopping and hyperparameter selection for all approaches.

**TFR Implementation.** We provide a TensorFlow Ranking implementation of the PiRank NDCG Loss as well as the original NeuralSort Permutation Loss which can be plugged in directly into TensorFlow Ranking.<sup>6</sup>

**Straight-through Estimation.** The PiRank surrogate learning objective can be optimized via two gradient-based techniques in practice. The default mode of learning is to use

the relaxed objective during both forward pass for evaluating the loss and for computing gradients via backpropagation. Alternatively, we could perform *straight-through estimation* [38], where we use the hard version (corresponding to the negative of the exact NDCG) for evaluating the loss forward, but use the relaxed objective in Eq. 9 for gradient evaluation. We observe improvements from the latter option and use it throughout.

**Architecture and Parameters.** Experiment parameters that are shared across methods, such as the scoring neural network architecture, batch size, training and test list sizes, are provided in Table 2. We did not rely on regularization, dropout or batch normalization in this work. Parameters specific to NeuralSort and PiRank are  $\tau = 5$  and  $d = 1$  across all experiments except for ablations (Section 4.2). The PiRank parameter based on NDCG cutoff  $k$  is fixed to 10 in all experiments. Parameters used for the baselines are the default setting of TensorFlow Ranking, with the exception of LambdaRank which uses  $k = 10$  for the Lambda weight.

**Experimental Workflow.** We rely on TensorFlow Ranking for most of our work outside the NeuralSort and PiRank loss implementations, which takes care of query grouping, document list tensor construction, baseline implementation and metric computation among others.

**Libraries and Software.** This work extensively relied on GNU Parallel [39] and the Sacred library<sup>7</sup> for experiments.

## D Ablation Experiments

We provide all results for the temperature experiments described in Section 4.2, in Figures 8, 9, 10, 11, 12, 5. The smoothing parameter used in all plots is 0.9, the number of data points is 100 epochs for all figures except the training loss (1,000 iterations). Full results for the ablation experiments on the training list size described in Section 4.2 are provided in Table 3.

## E Synthetic LTR Data

To the best of our knowledge, there is no public LTR dataset with very large numbers of documents per query ( $L > 1000$ ). We thus propose the following synthetic dataset for testing and development at scale (see Section 4.2):

For each query  $q_i$ ,  $i \in \{1, \dots, n\}$ ,

1. Generate  $L$  documents  $\{\mathbf{x}_{i,j}\}_{j=1}^L$  where  $\mathbf{x}_{i,j}$  is a vector of  $m_d$   $\phi$ -distributed document features.
2. Randomly pick a vector  $c_i$  of  $m_q \leq m_d$  column indices from  $\{1, \dots, m_d\}$  without replacement.
3. Generate  $\psi$ -distributed query features  $\{\gamma_i\}_{k=1}^{m_q}$ .
4. Compute labels capped between  $\ell$  and  $h$  s.t.  
 $y_{i,j} = \max(\ell, \min(h, \sum_{k=1}^{m_q} \gamma_k x_{i,j,c_k}))$ .
5. Concatenate the query features  $\{\gamma_i\}_{k=1}^{m_q}$  to each  $\mathbf{x}_{i,j}$ .

This process allows us to generate datasets of arbitrarily large size, where we control  $L$ ,  $n$ ,  $m$ ,  $c$  and the distributions  $\phi$  and  $\psi$ . The process is easy to reuse, and made available in our TFR codebase.

<sup>6</sup><https://github.com/ermongroup/pirank>

<sup>7</sup><https://github.com/IDSIA/sacred>

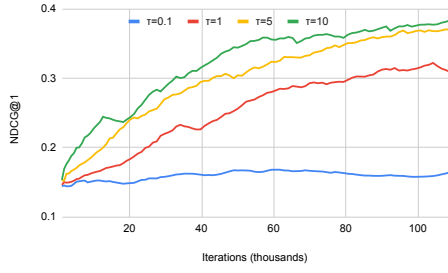


Figure 8: Validation NDCG@1 during PiRank training parametrized by temperature  $\tau$

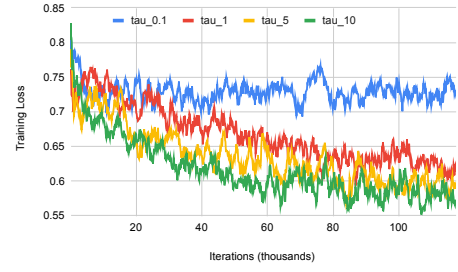


Figure 12: Training loss during PiRank training parametrized by temperature  $\tau$

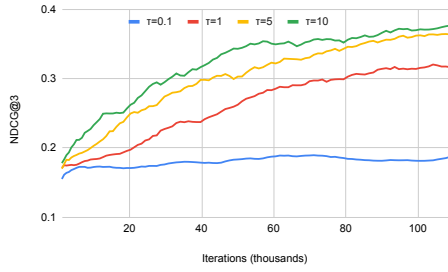


Figure 9: Validation NDCG@3 during PiRank training parametrized by temperature  $\tau$

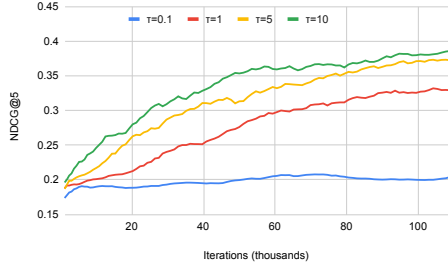


Figure 10: Validation NDCG@5 during PiRank training parametrized by temperature  $\tau$

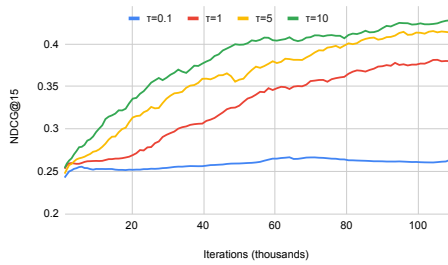


Figure 11: Validation NDCG@15 during PiRank training parametrized by temperature  $\tau$